

# A NOVEL DUAL-SIDE FABRICATION METHOD FOR SILICON PLATE SPRINGS WITH HIGH OUT-OF-PLANE STIFFNESS

J. Su<sup>1</sup>, H. W. van Zeijl<sup>1</sup>, S. L. Paalvast<sup>2</sup>, P. M. Sarro<sup>1</sup> and J. van Eijk<sup>2</sup>

<sup>1</sup>Delft University of Technology / DIMES, Feldmannweg 17, 2628CT Delft, Netherlands

<sup>2</sup>Delft University of Technology / 3mE, Mekelweg 2, 2628CD Delft, Netherlands

henkz@dimes.tudelft.nl

**Abstract** A high aspect ratio silicon plate spring is designed and fabricated in silicon using two novel technologies: dual side waferstepper alignment and deep reactive ion etching. The plate springs are characterized by resonance frequency measurements. A model of the plate spring is fitted to the measurement data to discriminate tolerances of the different technologies used in the fabrication process.

**Key Words:** dual side processing, Alignment, Deep Reactive Ion Etching, micro machined plate spring

## I INTRODUCTION

In precision engineering plate springs are commonly used construction elements for accurate guiding mechanisms. With the miniaturization of sensors and actuators the use of plate springs has been extended to the silicon micro domain (e.g. accelerometers, hard disk drive actuators and optical switches).

Modeling the plate spring (figure 1) as a slender beam, the stiffness in x-, y-, and z-direction can be approximated by [1]:

$$k_x = \frac{Eht}{l} \quad (1)$$

$$k_y = \frac{Eht^3}{4l^3} \quad (2)$$

$$k_z = \frac{Eth^3}{4l^3} \quad (3)$$

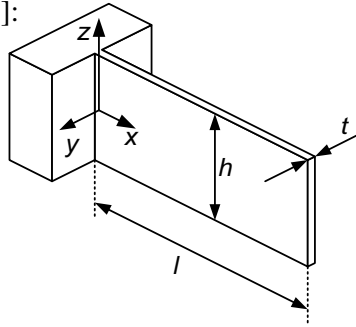


Figure 1. The vertical plate spring.

Here  $E$ ,  $h$ ,  $t$ , and  $l$  are the Young's modulus, the spring height, the spring thickness and the spring length.

When applied in a parallel guiding, the y-stiffness should be low, so the spring will be thin, long and  $h < l$ . As  $h^3/l^3 \ll 1$ , the stiffness in x-direction is inherently higher than in z-direction. In situations where we want to limit the influence of loading forces on the positioning accuracy, for example in a parallel guiding system (see figure 2a), the plate

spring should be used in an upright position (i.e. rotated 90° around the y-axis).

In this work, we studied a novel dual-side fabrication method to construct a plate spring orientated upright in a silicon wafer. Using this fabrication method, devices as shown in figure 2b are fabricated to characterize the plate springs

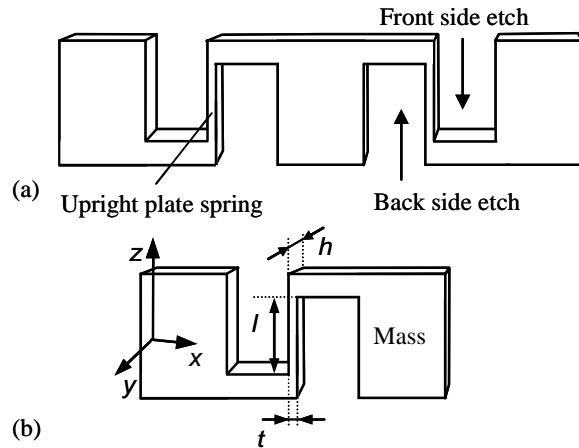


Figure 2. Schematic view of a parallel guiding with two upright plate springs (a) and the device fabricated in this work to characterize upright plate springs (b).

## II PROCESS DESCRIPTION

The fabrication of an upright plate spring-mass system as given in figure 2b requires two novel technologies; 3D-align<sup>TM</sup> and Deep Reactive Ion Etching (DRIE). 3D-align<sup>TM</sup> is an extension of the sub-micron alignment capabilities of an ASML waferstepper that allows Front-To-Backside wafer Alignment (FTBA). DRIE is used to etch deep cavities, aligned and etched on both sides of the wafer to form the upright plate spring.

Three lithographic masking layers are required to fabricate the upright plate spring-mass system. The used name and function of these layers are summarized in table 1 and the corresponding mask layout is shown in figure 3.

**Table 1. Lithographic layers to fabricate the upright plate spring.**

Layer name	Function
FC	Etch a cavity on the front side of the wafer.
BC	Etch a cavity on the back side of the wafer.
DRL	Release the device from the surrounding silicon by a through wafer etch.

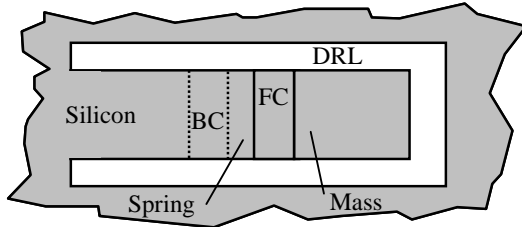
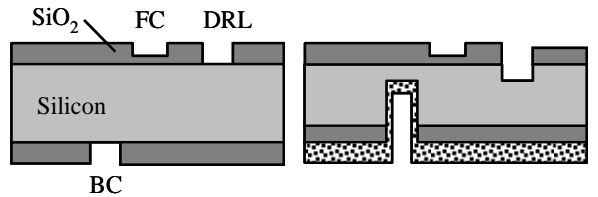
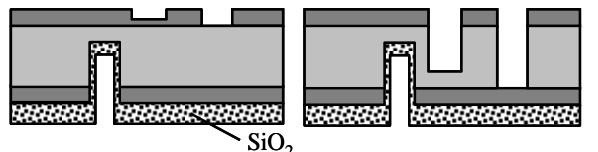


**Figure 3. Layout of the mass-spring system with upright springs.**

The process starts with the deposition of  $6\ \mu\text{m}$  PECVD silicon dioxide on both sides of a  $525\ \mu\text{m}$  thick,  $100\ \text{mm}$  double side polished silicon wafer. This oxide serves as a hard mask for the DRIE process. Both the BC and DRL layers are etched through the oxide, while the FC layer is partly etched (see figure 4a). All the required masking layers are etched in the masking oxide before any DRIE cavity is processed. This allows all the lithography steps to be completed using conventional wafer handling.



(a) Dual side processing of all the lithographic layers into the silicon oxide. (c) Partial etch of the DRL into the silicon.



(b) Etch the BC and deposit  $6\ \mu\text{m}$  silicon oxide on the backside of the wafer. (d) Remove the remaining FC oxide and etch the remaining silicon in the DRL areas.

**Figure 4. Device fabrication process flow.**

The BC areas are etched  $475\ \mu\text{m}$  deep into the backside of the wafer followed by a PECVD oxide deposition (figure 4b). This additional backside oxide prevents the under etching of the BC areas during the subsequent through wafer DRL etch.

Next the DRL is etched  $100\ \mu\text{m}$  into the silicon, the remaining FC oxide blocks the silicon etch in the FC areas (figure 4c). After the DRL silicon etch, the remaining FC oxide is removed using a maskless oxide RIE. In the next step, both the FC and DRL areas are further etched. This etch is continued until all the DRL silicon is removed (figure 4d). About  $75\ \mu\text{m}$  silicon is left in the FC areas to connect mass to the upright plate spring. In the last step the remaining oxide is removed using wet chemical etching.

### III FABRICATION TECHNOLOGY

FTBA accuracy plays a crucial role in the process described in the previous section. The designed thickness of the spring ( $t_0$ , see figure 5a) is directly affected by the front-to-backside alignment error ( $t_1$ , see figure 5b). The FTBA accuracy has been investigated in previous work [2] and is verified using FTBA calibration procedures [3]. The current FTBA accuracy on the ASML PAS5000/50 waferstepper, used in this work, is better than  $500\ \text{nm}$ .

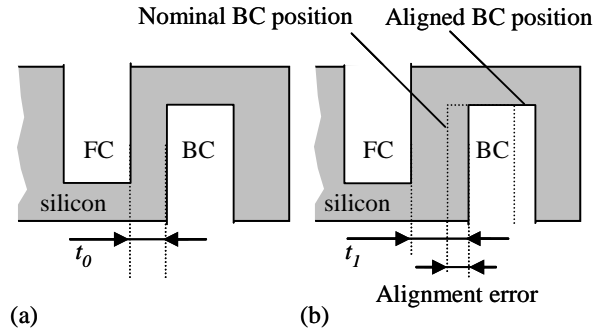


**Figure 5. The effect of an FTBA overlay error on the spring thickness.**

The effect of the DRIE process on the spring thickness is more complicated. In the first place the spring thickness is affected by the shape of the DRIE profile. For example, a positive side wall slope results in an increased thickness (see figure 6a), nevertheless, the thickness is constant over the entire length of the spring. Secondly, a non perpendicular direction of the DRIE profiles can affect the spring thickness in a non uniform way (see figure 6b).

Although DRIE offers high anisotropy for very deep structures, the profile direction might deviate from the ideal perpendicular direction. In our case, the etch depth is  $450\ \mu\text{m}$ . Consequently, a deviation of the ideal perpendicular direction of

only  $\pm 0.1$  degree will result in a displacement of  $\pm 0.8 \mu\text{m}$  at this depth.

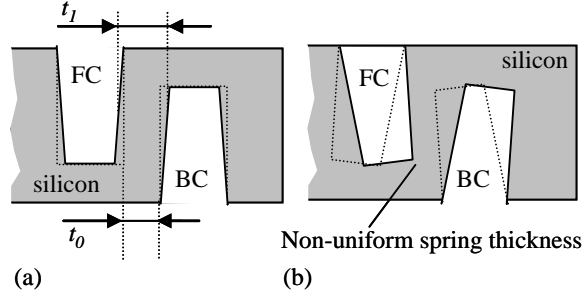


**Figure 6. The effect of a non-perpendicular etch profile on the spring thickness.**

The direction of the DRIE process can be investigated using electrical overlay measurements [4]. With this method, the front-to-back side overlay in a through wafer DRIE etch process is measured in the x-direction (see figure 7). Compared to the target spring thickness (10 - 20  $\mu\text{m}$ ), the measured overlay error is significant. Consequently the direction of the DRIE profile will have a significant influence on the spring thickness and uniformity.

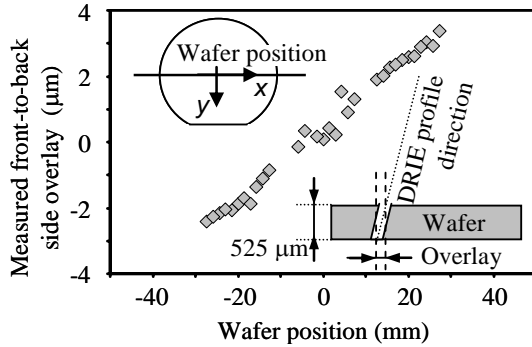


**Figure 7. Front-to-back side overlay error after through-wafer DRIE, measured across the wafer center.**

To discriminate the effect of FTBA and DRIE on the final spring thickness, the mass-spring devices are fabricated in closely spaced sets of mirrored and non-mirrored (reference) devices. The devices are mirrored in the x-direction.

Within one set, the distance between the two devices is less than 1 mm. Therefore we may assume that for both devices, the BC and FC DRIE profiles are similar. Therefore within one set, the influence of the DRIE process on the spring thickness is the same. However, within one set, a shift in the alignment error will introduce an asymmetrical change in the spring thickness (see figure 8). Thus the spring thickness of a set of

mirrored and reference devices can be described by two equations with two variables:

$$\text{Reference: } t_1 = t_0 + \Delta t_{etch} + \Delta t_{misalign} \quad (4)$$

$$\text{Mirrored: } t_1 = t_0 + \Delta t_{etch} - \Delta t_{misalign} \quad (5)$$

Here  $t_0$ ,  $\Delta t_{etch}$  and  $\Delta t_{misalign}$  are the desired spring thickness, the error caused by DRIE and error caused by FTBA misalignment, respectively.

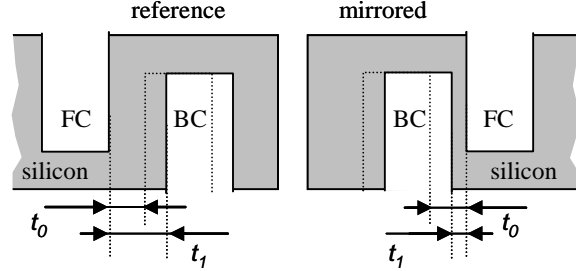


**Figure 8. The a-symmetrical effect of FC to BC alignment errors on the spring thickness.**

## IV MECHANICAL CHARACTERIZATION

Resonance frequency measurements are used to determine the stiffness of the plate springs, which is an important device parameter. From the stiffness the corresponding spring thickness can be calculated. But, in the case of non-uniform plate springs, this calculated thickness must be considered as an effective thickness, rather than a physical thickness. However, it can be shown analytically that the effective thickness is close to the thinnest part of the spring.

In this report, groups of mirrored and non-mirrored devices are characterized. The devices have different dimensions, such as spring height, mass size and cavity length, but within one group only the thickness is varied. The relation between the resonance frequency and stiffness is given by:

$$\omega^2 = \frac{k}{m} \quad (6)$$

To measure the resonance frequencies of the devices, the dies are mounted on a shaker. The mechanical response of our plate spring system to the shaker excitation is measured with a laser vibrometer. By determining the smallest frequency step which still resulted in a noticeable difference in amplitude, it was found that the frequency can be measured with an accuracy better than 10 ppm. We only consider the resonance mode where the mass is moving linear along the x-axis, because

this mode shape is similar to that of a plate springs in a parallel guiding. With the beam equations from [1], we can derive the equations describing the motion of the system, and analytically calculate the resonance frequency. After rewriting we find that the appropriate stiffness is approximated by:

$$k = \frac{Eht^3}{l^3} \quad (7)$$

The length of the spring depends on etch time and etch rate, but for devices within one set, the variation in length will be negligible. The same applies for variations in spring height and the mass ( $m$ ). And the Young's modulus is considered constant across a wafer. This means, that the resonance frequency of a set of devices depends on some constant factor and the actual thickness. Rewriting the resonance equation:

$$\omega^2 = \frac{k}{m} = \frac{Eht^3}{ml^3} = \frac{Eh}{ml^3} t^3 \Rightarrow \omega^2 = B^3 t^3 \quad (8)$$

$$\text{with } B = \left( \frac{Eh}{ml^3} \right)^{1/3} \quad (9)$$

$B$  might vary from its theoretical value, due to fabrication tolerances, so it is best calculated from the measurement results. Considering equation 4 and 5, the resonance frequencies for the reference and mirrored devices can be expressed as follow:

$$\text{reference: } \omega^{2/3} = B(t_0 + \Delta t_{etch} - \Delta t_{misalign}) \quad (10)$$

$$\text{mirrored: } \omega^{2/3} = B(t_0 + \Delta t_{etch} + \Delta t_{misalign}) \quad (11)$$

The three unknowns,  $B$ ,  $\Delta t_{etch}$  and  $\Delta t_{misalign}$ , cannot be solved with only two equations, but as process variations are very small within one group, a least squares fit can be used to extract the average values of these parameters. The results are discussed in section 5.

## V RESULT AND DISCUSSION

Three groups with sets of mirrored and reference devices are measured on three different locations across the wafer center (see figure 7). The dimensions of the spring within one group are:  $l = 400 \mu\text{m}$ ,  $h = 150 \mu\text{m}$  and  $t_0 = 10 - 20 \mu\text{m}$  in steps of  $2 \mu\text{m}$ . The results are summarized in table 2.

The variations in  $B$  are caused by the DRIE etch rate uniformity. The silicon etch rate of group I and III are 0.6 % higher compared with group II this

corresponds with the higher value for  $B$  for group II.

The fitted  $\Delta t_{misalign} < 0.4 \mu\text{m}$  which is within the specifications of the waferstepper, however  $\Delta t_{etch}$  varies considerably. The magnitude of these variations is close to the measured front-to-back side overlay as given in figure 7; evidently the direction of the DRIE profile has a profound influence on the effective plate spring thickness.

**Table 2. Fitted model parameters of 3 identical groups on different positions across the wafer center.**

Group number	Wafer position (mm)	$B$ ( $\text{m}^{-1}\text{s}^{-2/3}$ )	$\Delta t_{misalign}$ ( $\mu\text{m}$ )	$\Delta t_{etch}$ ( $\mu\text{m}$ )
I	-12	$1.79 \cdot 10^8$	0.15	-1.91
II	3	$1.87 \cdot 10^8$	0.38	-0.30
III	18	$1.80 \cdot 10^8$	0.08	-2.94

## VI CONCLUSIONS

High aspect ratio dual-side processed upright plate springs are successfully fabricated using two novel technologies; FTBA and DRIE. For these plate springs we found that FTBA accuracy is not the limiting factor. The non-perpendicular direction of the DRIE profile is mainly responsible for deviations of the spring thickness across the wafer.

## VII ACKNOWLEDGEMENTS

The authors would like to thank Dr. H. Krikhaar and W. de Laat from ASML for their support.

## REFERENCES

- [1] J.M. Gere and S.P. Timoshenko, *Mechanics of Materials*, London, Chapman & Hall, 3<sup>rd</sup> SI edition, pp.771-773, 1993.
- [2] H. W. van Zeijl, F. G. Bijnen, J. Slabbekoom, Characterization of waferstepper and process-related front-to backwafer overlay errors in bulk micromachining using electrical overlay test structures, *Proc. SPIE*, Vol. 5455, p. 398-406, Aug 2004.
- [3] E. M. Smeets, F. G. Bijnen, J. Slabbekoom, H. W. van Zeijl, 3D align overlay verification using glass wafers, Publication: *Proc. SPIE* Vol. 5641, p. 152-162, Dec. 2004
- [4] H. W. van Zeijl, J Slabbekoom, Characterization of front- to backwafer alignment and bulk micromachining using electrical overlay test structures, *Proc. SPIE* Vol. 5116, p. 617-626, Apr 2003.